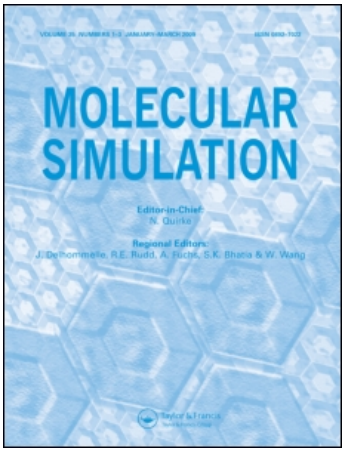

Molecular Simulation
Publication details, including instructions for authors and subscription information:
http://www.informaworld.com/smpp/title~content=t713644482

Microphase separation of star-diblock copolymer melts studied by dissipative particle dynamics simulation

Y. Xu[a]; J. Feng[b]; H. Liu[a]; Y. Hu[a]
[a] Department of Chemistry and Lab for Advanced Materials, East China University of Science and Technology, Shanghai, China [b] Department of Chemistry, Chuzhou University, Chuzhou, Anhui, China

To cite this Article Xu, Y. , Feng, J. , Liu, H. and Hu, Y.(2006) 'Microphase separation of star-diblock copolymer melts studied by dissipative particle dynamics simulation', Molecular Simulation, 32: 5, 375 — 383
To link to this Article: DOI: 10.1080/08927020600765003
URL: http://dx.doi.org/10.1080/08927020600765003

Molecular Simulation, Vol. 32, No. 5, 30 April 2006, 375–383

Taylor & Francis
Taylor & Francis Group

Microphase separation of star-diblock copolymer melts studied by dissipative particle dynamics simulation

Y. XU†, J. FENG†‡, H. LIU†* and Y. HU†

†Department of Chemistry and Lab for Advanced Materials, East China University of Science and Technology, Shanghai 200237, China
‡Department of Chemistry, Chuzhou University, Chuzhou, Anhui 239012, China

(Received January 2006; in final form April 2006)

The microphase-separation behaviors of two types of star-diblock copolymers $(A)_4(B)_4$ and $(AB)_4$ are investigated through the dissipative particle dynamics (DPD). The simulated phase diagrams show similar ordered mesostructures as those of corresponding linear and cyclic ones, such as lamellas (LAM), perforated lamellas (PL), hexagonal (HEX) cylinders and body-centered-cubic (BCC) spheres, besides, a series of gyroid (GR) morphologies predicted by theoretical research have been identified. In the regions between the totally ordered and disordered phases, we have found some melted morphologies that can be thought as locally ordered, such as micelles (M), liquid rods (LR) and random network (RN), which have not been identified in relevant theoretical predictions. The simulated threshold for a totally ordered mesostructure to appear is higher than theoretical predictions, which can be ascribed mainly to the increasing fluctuation with finite chain length, and the star architecture can facilitate microphase separation, which is in agreement with the theoretical predictions. In addition, it is easier for the $(A)_n(B)_n$ copolymers than for corresponding $(AB)_n$ ones to trigger microphase separation under the same conditions. The relations between the root-mean-square radius of gyration (RMSGR) and the composition f_A in the two types of star copolymers are almost contrary, which can be attributed to the differences in their structural characteristics.

Keywords: Microphase separation; Star diblock copolymer; Dissipative particle dynamics; Root-mean-square radius

1. Introduction

Block copolymers have received much attention over the past few decades due in a large part to their ability to form various ordered mesostructures arose from the variation of chain composition and external conditions. The chemically different constituents of the polymer usually tend to segregate, while the chemical connectivity prevents the segregation macroscopically, instead, the melts realize microphase-separation forming structures like lamellas (LAM), rods, spheres, bicontinuous structures [1,2], leading to novel properties and wide applications [3–8]. Understanding the microphase-separation behavior of block copolymers will contribute to utilizing them more effective and better.

Studies on linear diblock copolymers have made much progress as the topology is relatively simple. Linear triblock copolymers and nonlinear block copolymers with unique architectures, such as star, branch, graft, cyclic and comb shapes, have attracted less attention, especially in terms of computer simulation. The existed few simulation studies [9–18] are mostly based on traditional Monte-Carlo (MC) technique. Recently, by means of dissipative particle dynamics (DPD) method, Qian *et al.* [19] studied the microphase-separation behavior of cyclic diblock copolymer which could be compared with previous works [9]. For star block copolymers, the relevant syntheses [20–25] have been developed profoundly. It is valuable and highly expected to investigate the effect of the star architecture on physical properties, however, corresponding simulation studies are scarce [14,18].

In general, there are two types of star-diblock copolymers denoted by $(A)_n(B)_n$ and $(AB)_n$, respectively, schematically shown in figure 1. An $(A)_n(B)_n$ star copolymer is constructed by joining n identical linear diblock copolymers together at their A–B junction points, while an $(AB)_n$ is at the A chain ends. Each linear diblock copolymer contains N monomer units and the fraction of A segment is f. Therefore, an $(A)_n(B)_n$ star copolymer has $2n$ arms, each of the n arms contains fN A monomers and each of the other n arms contains $(1 - f)N$ B monomers, while an $(AB)_n$ star copolymer has n arms and each arm

*Corresponding author. Tel.: +86-21-64252921. Email: hlliu@ecust.edu.cn

Molecular Simulation
ISSN 0892-7022 print/ISSN 1029-0435 online © 2006 Taylor & Francis
http://www.tandf.co.uk/journals
DOI: 10.1080/08927020600765003

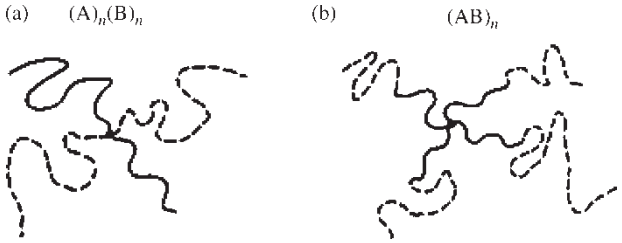

Figure 1. Schematic representation of two types of star-diblock copolymers.

is a whole linear A–B diblock chain. The total number of monomers in every star copolymer is $N_0 = nN$.

Olvera and Sanchez [26] have calculated the phase stability limit and static structure factors by mean-field theory near the order–disorder transition (ODT) for these systems, they have also derived the corresponding spinodals for systems with different numbers of arms. The results show that the spinodals for $(A)_n(B)_n$ are markedly symmetric, while for $(AB)_n$ they are asymmetric, consistent with the corresponding structural characteristic. In addition, the ODT critical values for $(AB)_n$ are smaller, indicating that the microphase separation is easier to occur for $(AB)_n$ than for $(A)_n(B)_n$. Matsen and Schick [27] have constructed phase diagrams for $(AB)_n$ by self-consistent-field (SCF) theory, showing that the systems can exhibit four kinds of microphase-separation structures: cubic, hexagonal (HEX), gyroid (GR) and lamellar micro-domains, similar to the behavior of linear diblock copolymers. Besides, the number of arms n has little influence on the form of the phase diagram. There are also other theoretical studies [28–31] and a considerable amount of experimental work [32–37] on these systems. However, comprehensive simulation studies are absent. We try to fill up this gap in this work.

2. Simulation method and model construction

The DPD method was first introduced by Hoogerbrugge and Koelman [38,39] and gradually improved by various auhors [40,41]. It has applied covering a wide fields and proved to be a versatile simulation technique for complex fluids on the mesoscopic scale such as polymer melts [19,42,43] and surfactant solutions [44–46]. Different from traditional MC and molecular dynamics (MD) methods, the elementary units in DPD are fluid elements or coarse grained soft particles representing a small region of fluid that contains a group of molecules. The time evolution is governed by Newton's equations of motion [41]

$$\frac{\mathrm{d}\,\mathbf{r}_i}{\mathrm{d}\,t} = \mathbf{v}_i, \quad \frac{\mathrm{d}\,\mathbf{v}_i}{\mathrm{d}\,t} = \mathbf{f}_i \tag{1}$$

For simplicity, the mass of each particle is set to 1, thus the force $\mathbf{f}_i$ acting on a particle i equals its acceleration $(\mathrm{d}\,\mathbf{v}_i)/(\mathrm{d}\,t)$, $\mathbf{v}_i$ is the velocity, $\mathbf{r}_i$ is the position vector. The interparticle interacting force $\mathbf{f}_i$ contains three parts; each of them is pairwise additive,

$$\mathbf{f}_i = \sum_{j \neq i} (\mathbf{F}_{ij}^{\mathrm{C}} + \mathbf{F}_{ij}^{\mathrm{D}} + \mathbf{F}_{ij}^{\mathrm{R}}) \tag{2}$$

The conservative force $\mathbf{F}_{ij}^{\mathrm{C}}$ is a soft repulsive force acting along the line of centers expressed as

$$\mathbf{F}_{ij}^{\mathrm{C}} = \begin{cases} a_{ij}(1 - r_{ij})\hat{\mathbf{r}}_{ij} & (r_{ij} < r_{\mathrm{C}} = 1) \\ 0 & (r_{ij} \geq r_{\mathrm{C}} = 1) \end{cases} \tag{3}$$

where a_{ij} is a maximum repulsion between particle i and j, $\mathbf{r}_{ij} = \mathbf{r}_i - \mathbf{r}_j$, $r_{ij} = |\mathbf{r}_{ij}|$, $\hat{\mathbf{r}}_{ij} = \mathbf{r}_{ij}/|\mathbf{r}_{ij}|$. The cutoff radius r_{c} is treated as a length unit.

The dissipative force $\mathbf{F}_{ij}^{\mathrm{D}}$ and the random force $\mathbf{F}_{ij}^{\mathrm{R}}$ act as heat sink and source, respectively, their combined effect is therefore a thermostat. They are given by

$$\begin{aligned} \mathbf{F}_{ij}^{\mathrm{D}} &= -\gamma\omega^{\mathrm{D}}(r_{ij})(\hat{\mathbf{r}}_{ij} \bullet \mathbf{v}_{ij})\hat{\mathbf{r}}_{ij}, \\ \mathbf{F}_{ij}^{\mathrm{R}} &= \sigma\omega^{\mathrm{R}}(r_{ij})\zeta_{ij}\Delta t^{-1/2}\hat{\mathbf{r}}_{ij} \end{aligned} \tag{4}$$

where ω^{D} and ω^{R} are r-dependent weigh functions and $\mathbf{v}_{ij} = \mathbf{v}_i - \mathbf{v}_j$. The ζ_{ij} is a random variable with zero mean and unit variance. Español and Warren have shown the relations between the two weigh functions as [40]

$$\omega^{\mathrm{D}}(r) = [\omega^{\mathrm{R}}(r)]^2 \quad \sigma^2 = 2\gamma k_{\mathrm{B}} T \tag{5}$$

where T is the absolute temperature and k_{B} is the Boltzmann constant. This relationship is established to satisfy the fluctuation–dissipation theorem, so that the system can ensure (angular) momentum conservation leading to an accurate description of hydrodynamics [47], the DPD method can therefore produce a correct canonical (*NVT*) ensemble [40]. In most relevant researches, a simple choice of the weigh functions is used,

$$\omega^{\mathrm{D}}(r) = [\omega^{\mathrm{R}}(r)]^2 = \begin{cases} (1 - r)^2 & (r < r_{\mathrm{C}} = 1) \\ 0 & (r \geq r_{\mathrm{C}} = 1) \end{cases} \tag{6}$$

The integration scheme of motion equations has a significant influence on the efficiency and reliability of the simulations. In DPD method, the dissipative forces and the relative velocities of the particles depend on each other, so the traditional Verlet algorithm commonly used in MD is not applicable. To overcome this difficulty, many integration schemes [41,48–50] have been proposed during the past few years, among them the modified velocity-Verlet integrator developed by Groot and Warren (GW-VV) [41] has been proved relatively efficient [19]

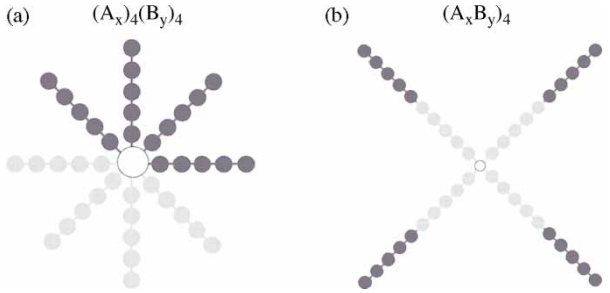

Figure 2. DPD models of two types of star-diblock copolymers. The gray and black particles represent the A and B blocks, respectively. The central jointing blank round represents a particle C.

and most widely applied. We adopt it in this work:

$$\begin{aligned}
\mathbf{r}_i(t+\Delta t) &= \mathbf{r}_i(t) + \Delta t \mathbf{v}_i(t) + \frac{1}{2}(\Delta t)^2 \mathbf{f}_i(t) \\
\tilde{\mathbf{v}}_i(t+\Delta t) &= \mathbf{v}_i(t) + \lambda \Delta t \mathbf{f}_i(t) \\
\mathbf{f}_i(t+\Delta t) &= \mathbf{f}_i(\mathbf{r}(t+\Delta t), \tilde{\mathbf{v}}(t+\Delta t)) \\
\mathbf{v}_i(t+\Delta t) &= \mathbf{v}_i(t) + \frac{1}{2}\Delta t(\mathbf{f}_i(t) + \mathbf{f}_i(t+\Delta t))
\end{aligned} \tag{7}$$

The star-diblock copolymers in simulations are modeled according to the sketches demonstrated in figure 1. As shown in figure 2, each star monomer is constructed by four identical linear A–B diblock free chains jointed together through a central particle C which is considered to be similar to either of the blocks. The copolymer is expressed as $(A_x)_4(B_y)_4$ and $(A_xB_y)_4$; a single linear chain consists of ten soft particles with the same diameter r_c, thus $N = x + y = 10$. The soft particles in a chain are connecting one by one via the harmonic springs with a spring force $\mathbf{F}_{ij}^S = C\mathbf{r}_{ij}$. The initial linking bond lengths between the neighboring particles are all set equal to unit length. In this work, we adopted a 3D simulation cell with periodic boundary conditions applied in all three directions. The number density ρ equals to 3 and the total number of particles in the system is 24,600, corresponding number of star copolymers is 600. The side of the simulation box is a little longer than 20. Referring to literature work [19,42,43], we chose the relevant parameters as $k_BT = 1$, $\sigma = 3.67$, $\lambda = 0.65$, $\Delta t = 0.06$ and $C = 4$. For simplicity, the reduced temperature of the whole system in next sections is denoted as T.

For comparing with corresponding theoretical work [26,27], we focused mainly on how the chain composition of block A, f_A, and the energy parameter χN influence the final mesoscopic ordered structures of the system. For the $(A_x)_4(B_y)_4$ and $(A_xB_y)_4$ copolymers, $f_A = x/(x+y)$. The Flory-Huggins χ parameter characterizing the interaction between A and B blocks can be chosen appropriately within a certain range and transformed into the most important interaction parameter in DPD via the linear mapping relation established by Groot and Warren [41,42],

$$a_{ij} \approx a_{ii} + 3.27\chi_{ij} \quad (\rho = 3) \tag{8}$$

where α_{ii} is the interacting energy between particles of the same type and in general $\alpha_{ii} = 25$. The C–A and C–B interacting energies are also taken as 25, because the central jointing particle C is considered to be similar to either of the block particles.

There is a possible doubt whether the simulation box is large enough to avoid the finite box size effect, which may help to induce ordering. Although in a mixture of two homopolymers, equilibrium phase separation occurs on a macroscopic size scale, while in block copolymers it can only occur on size scales of the order of the radius of gyration of the copolymer [26]. In our systems, the simulated root-mean-square radius of gyration (RMSGR) ranges from about 1.74 to 2.71 as the parameters f_A and χN vary, the side length of our simulation box is at least 7 times larger than it indicating that the finite box size effect may have no influence on our results.

3. Simulation results and discussion

3.1 Phase diagrams of $(A)_4(B)_4$ and $(AB)_4$ star copolymers

We have obtained a series of mesostructures by varying the composition f_A and the A–B interaction parameter χ. Phase diagrams of $(A)_4(B)_4$ and $(AB)_4$ star copolymers with χN as ordinate and f_A as abscissa are shown in figure 3. The phase diagram of $(A)_4(B)_4$ is distinctly symmetric compared to that of $(AB)_4$ in accord with the respective structural characteristic and the calculated results from mean-field theory [26]. From the initiation of ordered structures (solid symbols), the microphase separation seems to be easier for the $(A)_n(B)_n$ than for the $(AB)_n$ to occur, which is in contrary to the theoretical predictions [26]. For the $(AB)_n$ star copolymers, as the number of arms (n) increases, it may develop a "core and shell" type structure, where the core is rich in A and the shell is rich in B even in the disordered state. However, in this work, the number of arms is too small; the "core and shell" effect is not serious. We can see from figure 2 that the A and B segments are entirely separate in each arm of $(A)_n(B)_n$, while in $(AB)_n$ they are mixed in each arm. Therefore, compared to $(AB)_n$, the $(A)_n(B)_n$ star copolymers are easier to carry out microphase separation under the same conditions. This phenomenon is left for experimental verification.

3.2 General feature of the phase diagram

As a whole, the microphase-separation behavior of the two types of star-diblock copolymers, especially the $(A)_4(B)_4$ copolymers, are analogous to those of corresponding linear [51,52] and cyclic [19,53] diblock copolymers derived from theories and simulations. When the A–B

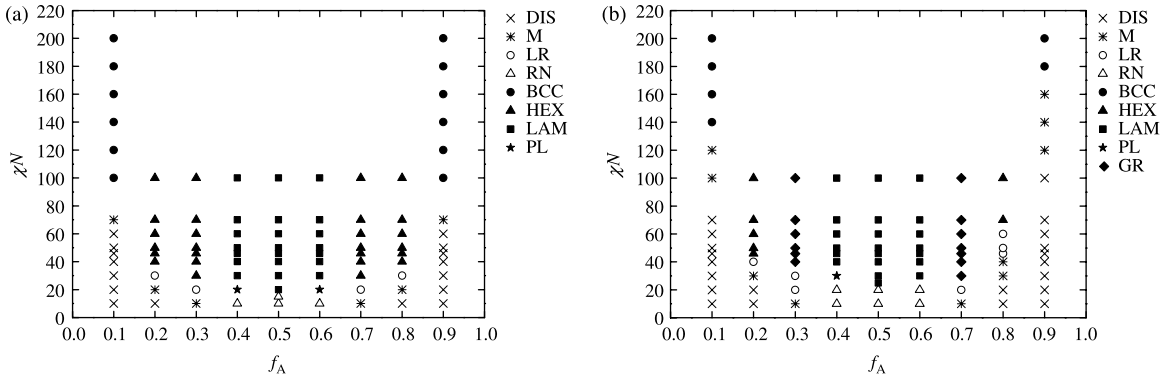

Figure 3. Simulated phase diagrams for the $(A)_4(B)_4$ and the $(AB)_4$ star-diblock copolymers. Disordered phase (DIS), Micelles (M), Liquid Rods (LR), Random Network (RN), Body-Centered-Cubic spheres (BCC), Hexagonal Cylinders (HEX), Lamellas (LAM), Perforated Lamellas (PL) and Gyroid (GR) are displayed.

interaction is relatively weak with smaller χ, the system shows totally disordered state. As the interaction strengthens gradually, a sequence of transitions will occur. If the copolymers are symmetric or moderately asymmetric ($f_A = 0.4 \sim 0.6$), LAM are usually the preferring morphologies, as shown in figure 4a. For highly asymmetric copolymers ($f_A = 0.1 \sim 0.3, 0.7 \sim 0.9$), HEX cylinders or BCC spheres are stable structures, as shown in figure 4b and c, respectively. In addition, we have observed a series of bicontinuous gyroidal morphologies formed by the $(AB)_4$ systems at $f_A = 0.3$ and $f_A = 0.7$, as shown in figure 4d. The SCF theory predicts that both the $(AB)_3$ and $(AB)_5$ systems are likely to form gyroidal structures when the composition fraction of either block is 0.3 [27], this is in accordance with our results. Another mesoscopic morphology that deserves attention is the perforated lamellar (PL) structures formed in the $(A_4)_4(B_6)_4$ or $(A_6)_4(B_4)_4$ system at $\chi N = 20$ and the $(A_4B_6)_4$ system at $\chi N = 30$, as shown in figure 5a and b, respectively. This morphology has never appeared in theoretical predictions, however, it is often observed through computer simulations [19,42,52], which can be regarded as an complementarity to relevant results from theoretical predictions.

3.3 Transition regions

In the phase diagrams from theoretical studies, the transition from one totally ordered phase to its neighbor is a sudden change, but the simulated results show there are transition regions. From figure 3, we can see that between the totally ordered and disordered phases there are some melted morphologies, such as micelles (M), liquid rods (LR) and random network (RN), which can be thought as locally ordered structures, as shown in figure 6. These morphologies have been identified by Groot *et al.* [43] and Qian *et al.* [19] in the DPD simulations on the microphase-separation behaviors of linear and cyclic diblock copolymers, respectively. Groot *et al.* have distinguished the formation processes of copolymer mesostructures on three different length and time scales [43], afterwards, Qian *et al.* have related these processes to the transitional morphologies from simulations [19]. Thus, it can be seen that their existence is very reasonable.

3.4 Further comparisons with the theoretical predictions

On the basis of mean-field theory, Olvera and Sanchez [26] have derived the ODT critical values for both types of star-diblock copolymers of infinitely long Gaussian chain. The calculated $(\chi N)_{\text{infinite}}$ equals 10.5 and 7.07 for the $(A)_4(B)_4$ and $(AB)_4$ at $f = 0.5$, respectively. This value can also be approximately located in our simulated phase diagrams in figure 3. We can easily see that it is between 15.0 and 20.0 for the $(A_5)_4(B_5)_4$ and in the range of $20.0 < (\chi N)_{\text{ODT}} < 25.0$ for the $(A_5B_5)_4$, both are larger than the theoretical predictions. Figure 7a and b shows

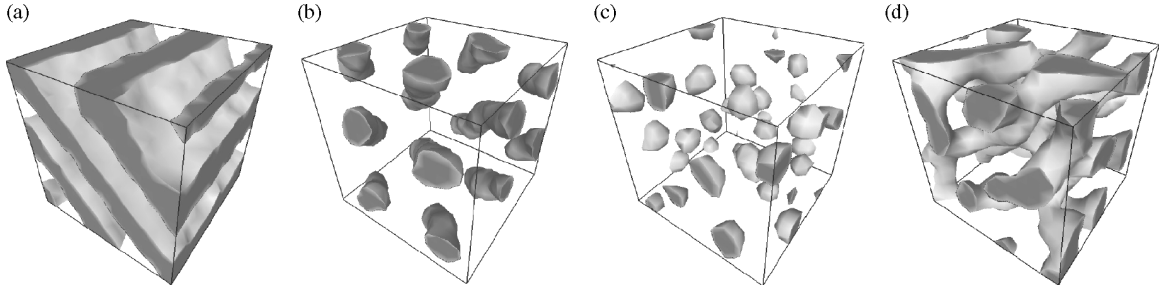

Figure 4. Typical simulated totally ordered mesoscopic structures for the star-diblock copolymers. (a) LAM formed by $(A_5B_5)_4$ at $\chi N = 100$; (b) HEX formed by $(A_2)_4(B_8)_4$ at $\chi N = 100$; (c) BCC formed by $(A_1)_4(B_9)_4$ at $\chi N = 200$; (d) GR formed by $(A_7B_3)_4$ at $\chi N = 70$.

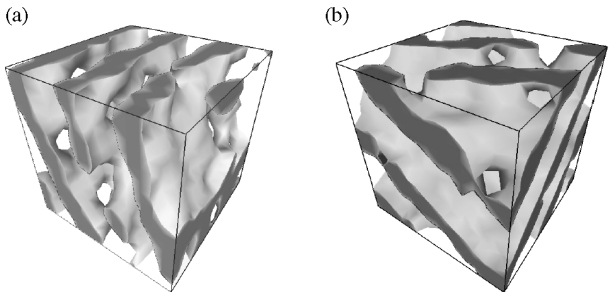

Figure 5. PL structures formed in different systems. (a) PL formed by $(A_4)_4(B_6)_4$ and $(A_6)_4(B_4)_4$ at $\chi N = 20$; (b) PL formed by $(A_4B_6)_4$ at $\chi N = 30$.

another rough comparison of the microphase-separation behaviors between the DPD simulation results for $(AB)_4$ star-diblock copolymers (symbols) of this work and the predictions by SCF theory for $(AB)_3$ and $(AB)_5$ star-diblock copolymers (solid lines) [27], respectively. Although the numbers of arms are a little different between them, the comparison is still meaningful because the number of arms has little influence on the phase diagrams. Apart from the transition phases mentioned above, an evident difference is that the simulated threshold for appearing a phase is higher than that of the theoretical prediction. For example, the SCF theory predicts that both $(A_5B_5)_3$ and $(A_5B_5)_5$ systems form lamellar phases when $\chi N = 20$, the DPD simulation shows it still remains in the RN phase when $\chi N = 20$, the system will not form the expected lamellar phase until $\chi N = 30$. The threshold for the LAM is higher than the SCF prediction. Groot *et al.* [42] and Qian *et al.* [19] have found analogous deviations when investigating by the DPD method the microphase-separation behaviors of linear and cyclic diblock copolymers, respectively. This discrepancy can be ascribed basically to the increasing fluctuation with finite chain length adopted in the simulations, which lacks Gaussian statistics assumed generally in relevant theories. Fredrickson and Helfand [54] have shown by weak coupling calculations that the ODT critical value for small linear diblock copolymers at $f = 0.5$ is $(\chi N)_{\mathrm{ODT}} = 10.495 + 41.022N^{-1/3}$, following from which Groot *et al.* [42] have given an expression for relating the simulated finite chain χN with that of the infinitely long chain predicted by theories, $(\chi N)_{\mathrm{infinite}} = (\chi N)_{\mathrm{ODT}}/(1 + 3.9N^{2/3-2\nu})$. Afterwards, by means of a chain length mapping from cyclic diblock copolymers to corresponding linear ones, Qian *et al.* [19] have successfully applied this formula to prove the simulated ODT critical value for the symmetric case. It is very easy for us to follow their treatment to obtain the ODT critical values for star diblock copolymers and the calculated $(\chi N)_{\mathrm{ODT}}$ is 21.4 and 13.5 for the $(A_5)_4(B_5)_4$ and $(A_5B_5)_4$, respectively, both disagree with our simulated results indicating this method is not applicable for the star diblock copolymers and another better analytic technique is to be developed to interpret quantitatively this disagreement, especially for the asymmetric cases. There is still one qualitative point we can make sure that the longer the chain length adopted in simulations is, the less the difference between theoretical predictions and simulated results is, especially in the ODT point, whereas, simultaneously the more the required simulation cost is.

Studies based on computer simulation [19] and experiments [55] have indicated that the organized microphase-separation structures of cyclic diblock copolymers differ remarkably from those of corresponding linear ones under the same conditions. The comparison between star-diblock copolymers and corresponding linear ones is also interesting. Figure 8a and b shows the differences in microphase-separation behaviors between the predictions by SCF for AB linear diblock copolymers (solid lines) [27] and the DPD simulation results for $(A)_4(B)_4$ and $(AB)_4$ star-diblock copolymers (symbols), respectively. Detailed comparisons are listed in table 1a—d, where the results for linear AB diblock copolymers at $\chi N = 46$ in table 1b are consistent with Groot and Madden's simulations [42]. It may think that the star architecture could prevent the microphase separation. However, an intuitive and significant information we draw from these tables is that the microphase separation is easier for the star-diblock copolymers than that of the corresponding linear ones under the same conditions, and the $(A)_4(B)_4$ copolymers are more superior. For example, the star $(A_1)_4(B_9)_4$ forms an ordered phase BCC at $\chi N = 100$, while the star $(A_1B_9)_4$ only forms a locally

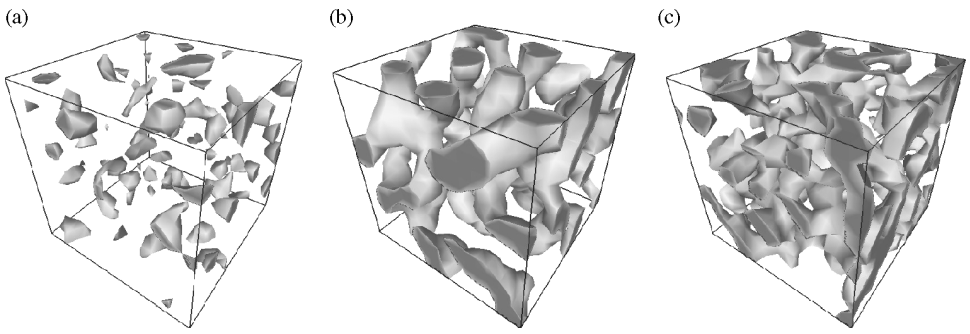

Figure 6. Typical simulated locally ordered mesoscopic structures for the star-diblock copolymers. (a) M formed by $(A_8B_2)_4$ at $\chi N = 30$; (b) LR formed by $(A_3B_7)_4$ at $\chi N = 30$; (c) RN formed by $(A_4)_4(B_6)_4$ at $\chi N = 10$.

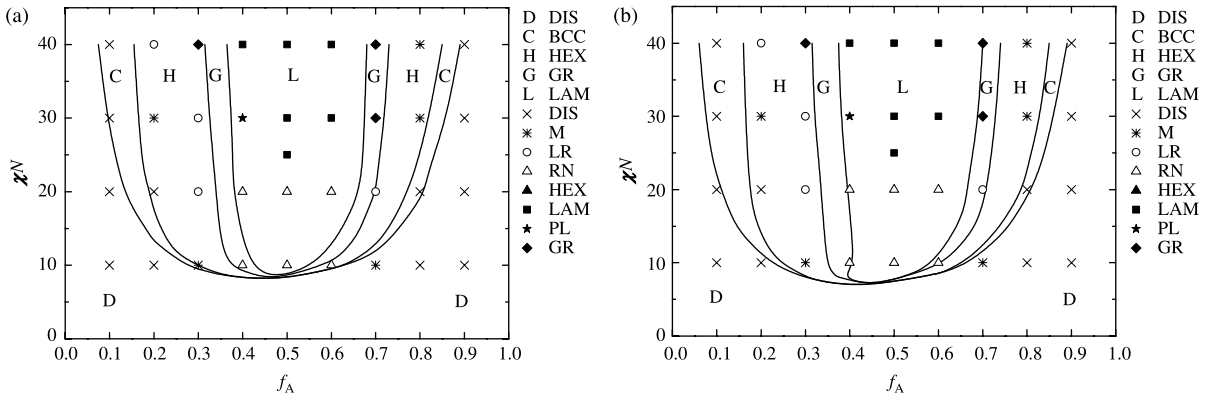

Figure 7. Comparison of the microphase-separation behaviors between the DPD simulation results for $(AB)_4$ star-diblock copolymers (symbols) and the predictions from SCF theory for $(AB)_3$ (a) and $(AB)_5$ (b) star-diblock copolymers (solid lines) [27], respectively.

ordered phase M, and the linear A_1B_9 just stays in the disordered state. We can reach a conclusion that the star architecture is favorable for microphase separation, which is in agreement with the predictions by mean-field [26] and SCF theories [27].

3.5 Radius of gyration

A curly polymer chain in a mesoscopic system can be imaged as an irregular ball and its microscopic morphology can be characterized effectively through its radius of gyration. We study the RMSGR defined by

$$\left(\langle R_g^2\rangle\right)^{0.5} = \left(\langle \frac{1}{M}\sum_{i=1}^{M}\left(|\mathbf{r}_i - \mathbf{r}_{cm}|\right)^2\rangle\right)^{0.5} \qquad (9)$$

where M is the number of particles in a star chain, $\mathbf{r}_i$ and $\mathbf{r}_{cm}$ denote the position vector of each particle in a star chain and the center of mass for the whole star chain, respectively. As shown in figure 2, particles in a $(A)_4(B)_4$ star chain are more centralized comparing to those in a $(AB)_4$ star chain, the RMSGR of the former should be smaller. Figure 9 demonstrates the variations of RMSGR with the composition f_A and the interaction parameter χN in the two types of star copolymers, from which we can see that even the maximum of RMSGR in the $(A)_4(B)_4$ systems approximates to the minimum of RMSGR in the $(AB)_4$ systems. Generally, the RMSGR increases as the A–B interaction strengthens. This is because that stronger repulsion between different segments can make the polymer chain more stretched, thus the imaginary polymer ball is bigger.

On the composition dependence, when the A–B interaction is relatively weak or moderate, as f_A changes from 0.1 to 0.9, the value of RMSGR in an $(A)_4(B)_4$ system decreases to a minimum first, then increases symmetrically. Referring to figure 2, when the structure of an $(A)_4(B)_4$ copolymer is asymmetric, the particles in it will be relatively distant from the center of mass, thus the value of RMSGR is large. As the structure becomes more symmetric, the component particles will be comparatively near the center of mass, the value of RMSGR decreases naturally and reaches the minimum at $f_A = 0.5$. Meanwhile, as mentioned above, the reinforcing of A–B interaction increases the RMSGR. As a combined effect, apparently abnormal ascending trends in the curves of $\chi N = 70$ and $\chi N = 100$ occur. As for the $(AB)_4$ systems, when f_A becomes relatively comparable to f_B, the number of possible A–B interaction pairs increases causing the increase of RMSGR. The stronger the A–B interaction,

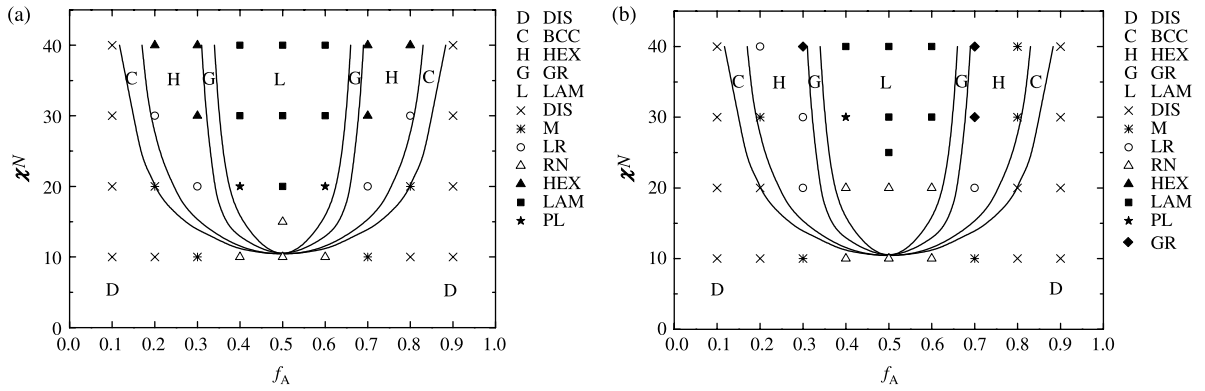

Figure 8. Comparison of the microphase-separation behaviors between the predictions from SCF theory for AB linear diblock copolymers (solid lines) [27] and the DPD simulation results for $(A)_4(B)_4$ (a) and $(AB)_4$ (b) star-diblock copolymers (markers), respectively.

Table 1. Comparison between star and corresponding linear diblock copolymers.

	Systems and phases		
f_A	$(A)_4(B)_4$	$(AB)_4$	AB
(a) $\chi N = 30$			
0.1	DIS	DIS	DIS
0.2	LR	M	M
0.3	HEX	LR	LR
0.4	LAM	PL	RN
0.5	LAM	LAM	LAM
0.6	LAM	LAM	RN
0.7	HEX	GR	LR
0.8	LR	M	M
0.9	DIS	DIS	DIS
(b) $\chi N = 46$			
0.1	DIS	DIS	DIS
0.2	HEX	HEX	M
0.3	HEX	GR	HEX
0.4	LAM	LAM	LAM
0.5	LAM	LAM	LAM
0.6	LAM	LAM	LAM
0.7	HEX	GR	HEX
0.8	HEX	LR	M
0.9	DIS	DIS	DIS
(c) $\chi N = 70$			
0.1	M	DIS	DIS
0.2	HEX	HEX	HEX
0.3	HEX	GR	HEX
0.4	LAM	LAM	LAM
0.5	LAM	LAM	LAM
0.6	LAM	LAM	LAM
0.7	HEX	GR	HEX
0.8	HEX	HEX	HEX
0.9	M	DIS	DIS
(d) $\chi N = 100$			
0.1	BCC	M	DIS
0.2	HEX	HEX	HEX
0.3	HEX	GR	HEX
0.4	LAM	LAM	LAM
0.5	LAM	LAM	LAM
0.6	LAM	LAM	LAM
0.7	HEX	GR	HEX
0.8	HEX	HEX	HEX
0.9	BCC	DIS	DIS

i.e. the larger χN, the more prominent this effect is. The asymmetry in the curves is owing to the structures.

4. Conclusions

The microphase-separation behaviors of two types of star-diblock copolymers $(A)_4(B)_4$ and $(AB)_4$ are investigated through the DPD by varying the composition f_A and the A–B interaction parameter χ. The simulated phase diagrams show similar ordered mesostructures as those of corresponding linear and cyclic ones, which exhibit LAM, perforated lamellas (PL), HEX cylinders and body-centered-cubic (BCC) spheres, besides, a series of GR morphologies predicted by theoretical research have been identified.

In the regions between the ordered and disordered phases, we have found some melted morphologies, such as μ, LR and RN, which can be thought as locally ordered. These morphologies have also appeared in the DPD simulations of linear and cyclic diblock copolymers. They can be regarded as transition phases, which have not been identified in relevant theoretical predictions.

The simulated threshold for a totally ordered mesostructure to appear is higher than theoretical predictions, which can be attributed chiefly to the increasing fluctuation with finite chain length adopted in the simulations, and a better analytic approach is to be developed to account quantitatively for this discrepancy.

Through comparing the microphase-separation behaviors of star-diblock copolymers and corresponding linear ones, we have found that the star architecture facilitates microphase separation, which is in accordance with the theoretical predictions. In addition, it is easier for the $(A)_n(B)_n$ copolymers than for corresponding $(AB)_n$ ones to trigger microphase separation under the same conditions.

The relations between the RMSGR and the composition f_A in the two types of star copolymers are almost contrary, which can be attributed to the differences in their structural characteristics.

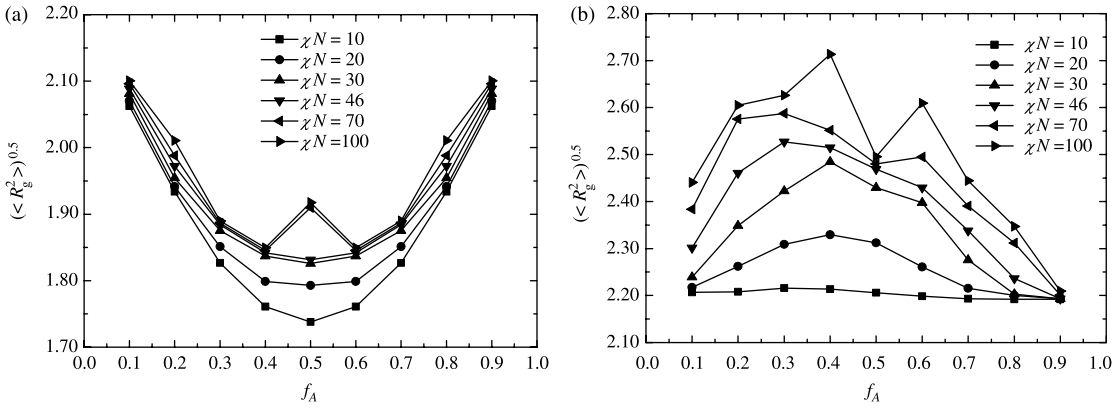

Figure 9. Variations of RMSGR with the composition f_A at different A–B interactions in the $(A)_4(B)_4$ (a) and $(AB)_4$ (b) star systems, respectively.

Acknowledgement

This work is supported by the National Natural Science Foundation of China (Projects No. 20236010, 20476025, 20490200), E-Institute of Shanghai High Institution Grid (No.200303) and Shanghai Municipal Education Commission of China.

References

[1] F.S. Bates, G.H. Frederickson. Block copolymer thermodynamics—theory and experiment. *Annu. Rev. Phys. Chem.*, **41**, 525 (1990).
[2] F. Corberi, G. Gonnella, A. Lamura. Two-scale competition in phase separation with shear. *Phys. Rev. Lett.*, **83**, 4057 (1999).
[3] W.A. Lopes, H.M. Jaeger. Hierarchical self-assembly of metal nanostructures on diblock copolymer scaffolds. *Nature (Lond.)*, **414**, 735 (2001).
[4] M. Templin, A. Franck, A. DuChesne, H. Leist, Y.M. Zhang, R. Ulrich, V. Schadler, U. Wiesner. Organically modified aluminosilicate mesostructures from block copolymer phases. *Science*, **278**, 1795 (1997).
[5] L. Podariu, A. Chakrabarti. Block copolymer thin films on corrugated substrates. *J. Chem. Phys.*, **113**, 6423 (2000).
[6] T. Turn-Albrecht, J. Schotter, G.A. Kaestle, N. Emley, T. Shibauchi, L. Krusin-Elbaum, K. Guarini, C.T. Black, M.T. Tuominen, T.P. Russell. Ultrahigh-density nanowire arrays grown in self-assembled diblock copolymer templates. *Science*, **290**, 2126 (2000).
[7] M. Park, C. Harrison, P.M. Chaikin, R.A. Register, D.H. Adamson. Block copolymer lithography: periodic arrays of ~10 to the 11th power holes in 1 square centimeter. *Science*, **276**, 1401 (1997).
[8] I.W. Hamley. Nanostructure fabrication using block copolymers. *Nanotechnology*, **14**, R39 (2003).
[9] A. Weyersberg, T.A. Vilgis. Microphase separation in topologically constrained ring copolymers. *Phys. Rev. E*, **49**, 3097 (1994).
[10] G. Floudas, S. Pispas, N. Hadjichristidis, T. Pakula, I. Erukhimovich. Microphase separation in star block copolymers of styrene and isoprene: theory, experiment, and simulation. *Macromolecules*, **29**, 4142 (1996).
[11] W.H. Jo, S.S. Jang. Monte Carlo simulation of the order-disorder transition of a symmetric cyclic diblock copolymer system. *J. Chem. Phys.*, **111**, 1712 (1999).
[12] T. Dotera, A. Hatano, T. Gemma. Microphase separation morphology in multiblock copolymer melts obtained from Monte Carlo simulations. *Kobunshi Ronbunshu*, **56**, 667 (1999).
[13] V.V. Vasilevskaya, A.A. Klochkov, P.G. Khalatur, A.R. Khokhlov, G. ten Brinke. Microphase separation within a comb copolymer with attractive side chains: a computer simulation study. *Macromol. Theory Simul.*, **10**, 389 (2001).
[14] T. Gemma, A. Hatano, T. Dotera. Monte Carlo simulations of the morphology of ABC star polymers using the diagonal bond method. *Macromolecules*, **35**, 3225 (2002).
[15] J. Feng, E. Ruckenstein. The morphology of symmetric triblock copolymer melts confined in a slit: a Monte Carlo simulation. *Macromol. Theory Simul.*, **11**, 630 (2002).
[16] J. Feng, E. Ruckenstein. Monte Carlo simulation of triblock copolymer thin films. *Polymer*, **43**, 5775 (2002).
[17] C.Y. Shew, R.M. Peetz, J.Q. Wang. Monte Carlo simulation of orientation ordering in grafted rodlike polymers. *Polymer Preprints*, **45**, 812 (2004).
[18] J.R. Maury-Evertsz, L.A. Estevez, G.E. Lopez. A molecular interpretation of vitreous boron oxide dynamics. *J. Chem. Phys.*, **121**, 8562 (2004).
[19] H.J. Qian, Z.Y. Lu, L.J. Chen, Z.S. Li, C.C. Sun. Computer simulation of cyclic block copolymer microphase separation. *Macromolecules*, **38**, 1395 (2005).
[20] M. Liu, P.F. Britt, J.W. Mays. Synthesis of amphiphilic miktoarm star copolymer A_2B_2 of polystyrene and poly (ethylene oxide). *Polymer Preprints*, **45**, 555 (2004).
[21] J. Wei, J.L. Huang. Synthesis of an amphiphilic star triblock copolymer of polystyrene, poly(ethylene oxide), and polyisoprene using lysine as core molecule. *Macromolecules*, **38**, 1107 (2005).
[22] M. Shi, H.L. Zhang, J. Chen, X.Y. Wan, Q.F. Zhou. Synthesis and characterization of a novel star shaped rod-coil block copolymer. *Polymer Bull.*, **52**, 401 (2004).
[23] W.Z. Yuan, X.Z. Tang, X.B. Huang, S.X. Zheng. Synthesis, characterization and thermal properties of hexaarmed star-shaped poly(ε-caprolactone)-*b*-poly(d,l-lactide-*co*-glycolide) initiated with hydroxyl-terminated cyclotriphosphazene. *Polymer*, **46**, 1701 (2005).
[24] N. Kang, J.C. Leroux. Triblock and star-block copolymers of *N*-(2-hydroxypropyl)methacrylamide or *N*-vinyl-2-pyrrolidone and d,l-lactide: synthesis and self-assembling properties in water. *Polymer*, **45**, 8967 (2004).
[25] K. Min, M. Li, N.M. Jahed, K. Matyjaszewski. Synthesis of star block copolymers via SR&NI ATRP in miniemulsion. *Polymer Preprints*, **45**, 682 (2004).
[26] C.M. Olvera, I.C. Sanchez. Theory of microphase separation in graft and star copolymers. *Macromolecules*, **19**, 2501 (1986).
[27] M.W. Matsen, M. Schick. Microphase separation in starblock copolymer melts. *Macromolecules*, **27**, 6761 (1994).
[28] H. Benoit, G. Hadziioannou. Scattering theory and properties of block copolymers with various architectures in the homogeneous bulk state. *Macromolecules*, **21**, 1449 (1988).
[29] D.M. Anderson, E.L. Thomas. Microdomain morphology of star copolymers in the strong-segregation limit. *Macromolecules*, **21**, 3221 (1988).
[30] A.M. Mayes, C.M. Olvera. Microphase separation in multiblock copolymer melts. *J. Chem. Phys.*, **91**, 7228 (1989).
[31] A.V. Dobrynin, I.Ya. Erukhimovich. Computer-aided comparative investigation of architecture influence on block copolymer phase diagrams. *Macromolecules*, **26**, 276 (1993).
[32] D.B. Alward, D.J. Kinning, E.L. Thomas, L.J. Fetters. Effect of arm number and arm molecular weight on the solid-state morphology of poly(styrene-isoprene) star block copolymers. *Macromolecules*, **19**, 215 (1986).
[33] D.J. Kinning, E.L. Thomas, D.B. Alward, L.J. Fetters, D.L. Handlin Jr. Sharpness of the functionality-induced structural transition in poly (styrene-isoprene) star block copolymers. *Macromolecules*, **19**, 1288 (1986).
[34] E.L. Thomas, D.B. Alward, D.J. Kinning, D.C. Martin, D.L. Handlin Jr, L.J. Fetters. Ordered bicontinuous double-diamond structure of star block copolymers: a new equilibrium microdomain morphology. *Macromolecules*, **19**, 2197 (1986).
[35] D.S. Herman, D.J. Kinning, E.L. Thomas, L.J. Fetters. A compositional study of the morphology of 18-armed poly(styrene-isoprene) star block copolymers. *Macromolecules*, **20**, 2940 (1987).
[36] D.M.A. Buzza, I.W. Hamley, A.H. Fzea, M. Moniruzzaman, J.B. Allgaier, R.N. Young, P.D. Olmsted, T.C.B. McLeish. Anomalous difference in the order-disorder transition temperature comparing a symmetric diblock copolymer AB with its hetero-four-arm star analog A_2B_2. *Macromolecules*, **32**, 7483 (1999).
[37] M. Grigoris, M. Maria, P. Stergios. Micelles of star block $(PSPI)_8$ and PSPI diblock copolymers (PS=Polystyrene, PI=Polyisoprene): structure and kinetics of micellization. *Macromolecules*, **38**, 940 (2005).
[38] P.J. Hoogerbrugge, J.M.V.A. Koelman. Simulating microscopic hydrodynamic phenomena with dissipative particle dynamics. *Europhys. Lett.*, **19**, 155 (1992).
[39] J.M.V.A. Koelman, P.J. Hoogerbrugge. Dynamic simulations of hard-sphere suspensions under steady shear. *Europhys. Lett.*, **21**, 363 (1993).
[40] P. Español, P.B. Warren. Statistical mechanics of dissipative particle dynamics. *Europhys. Lett.*, **30**, 191 (1995).
[41] R.D. Groot, P.B. Warren. Dissipative particle dynamics: bridging the gap between atomistic and mesoscopic simulation. *J. Chem. Phys.*, **107**, 4423 (1997).
[42] R.D. Groot, T.J. Madden. Dynamic simulation of diblock copolymer microphase separation. *J. Chem. Phys.*, **108**, 8713 (1998).
[43] R.D. Groot, T.J. Madden, D.J. Tildesley. On the role of hydrodynamic interactions in block copolymer microphase separation. *J. Chem. Phys.*, **110**, 9739 (1999).
[44] R.D. Groot. Mesoscopic simulation of polymer-surfactant aggregation. *Langmuir*, **16**, 7493 (2000).
[45] S. Yamamoto, Y. Maruyama, S. Hyodo. Dissipative particle dynamics study of spontaneous vesicle formation of amphiphilic molecules. *J. Chem. Phys.*, **116**, 5842 (2002).

[46] S.L. Yuan, Z.T. Cai, G.Y. Xu. Mesoscopic simulation of aggregates in surfactant/oil/water systems. *Chin. J. Chem.*, **21**, 112 (2003).
[47] P. Español. Hydrodynamics from dissipative particle dynamics. *Phys. Rev. E*, **52**, 1734 (1995).
[48] G. Besold, I. Vattulainen, M. Karttunen, J.M. Polson. Towards better integrators for dissipative particle dynamics simulations. *Phys. Rev. E*, **62**, R7611 (2000).
[49] I. Vattulainen, M. Karttunen, G. Besold, J.M. Polson. Integration schemes for dissipative particle dynamics simulations: from softly interacting systems towards hybrid models. *J. Chem. Phys.*, **116**, 3967 (2002).
[50] T. Shardlow. Splitting for dissipative particle dynamics. *SIAM J. Sci. Comput.*, **24**, 1267 (2003).
[51] L. Leibler. Theory of microphase separation in block copolymers. *Macromolecules*, **13**, 1602 (1980).
[52] A.J. Schultz, C.K. Hall, J. Genzer. Computer simulation of copolymer phase behavior. *J. Chem. Phys.*, **117**, 10329 (2002).
[53] A.N. Morozov, J.G.E.M. Fraaije. Phase behavior of ring diblock copolymer melt in equilibrium and under shear. *Macromolecules*, **34**, 1526 (2001).
[54] G.H. Fredrickson, E. Helfand. Fluctuation effects in the theory of microphase separation in block copolymers. *J. Chem. Phys.*, **87**, 697 (1987).
[55] S. Lecommandoux, R. Borsali, M. Schappacher, A. Deffieux, T. Narayanan, C. Rochas. Microphase separation of linear and cyclic block copolymers poly (styrene-*b*-isoprene): SAXS experiments. *Macromolecules*, **37**, 1843 (2004).